

Dynamical behaviour of a statistical manifold associated with correlated walks

This article has been downloaded from IOPscience. Please scroll down to see the full text article.

1994 J. Phys. A: Math. Gen. 27 5715

(<http://iopscience.iop.org/0305-4470/27/17/009>)

View [the table of contents for this issue](#), or go to the [journal homepage](#) for more

Download details:

IP Address: 171.66.16.68

The article was downloaded on 01/06/2010 at 23:03

Please note that [terms and conditions apply](#).

Dynamical behaviour of a statistical manifold associated with correlated walks

Tsunehiro Obata†, Hiroaki Hara‡ and Kunio Endo§

† Department of Electrical Engineering, Faculty of Engineering, Tohoku University, Sendai 980, Japan

‡ Department of Engineering Science, Faculty of Engineering, Tohoku University, Sendai 980, Japan

§ Japan Weather Association, Aoba-ku Sendai 980, Japan

Received 19 July 1993, in final form 15 February 1994

Abstract. A Riemann space associated with a correlated walk (cw) model is investigated by a numerical method, which is applicable to many other stochastic processes. The behaviour of the Riemann curvature is shown to have a close relation to the stability of the cw system. The Riemann space is spanned by two parameters representing jump probabilities of the cw model. The cw manifold evolves through some characteristic eras: it starts at a point, and changes to a line, and then to a homogeneous spherical surface of the scalar curvature $R = \frac{1}{2}$. The homogeneous space immediately transforms to an inhomogeneous space. The inhomogeneity gradually grows: a region of the inhomogeneous space violently oscillates in time and another region expands fast. As a whole, the curvature of the space decreases and soon becomes negative. The oscillations have already started to fade away. The negative curvature goes on decreasing and finally the space converges to a homogeneous saddle surface of $R = -1$. Such a behaviour of the curvature is shown to be well understood by the terms of ‘stability’ and ‘order parameter’ of stochastic processes. In other words, the inhomogeneity, the oscillation, and the decrease behaviour of the curvature are closely related to stability and orderliness of the correlated system.

1. Introduction

A parametrized family $S = \{p(x, \theta)\}$ of probability distributions is often treated in statistical inference, where x is a random variable and $\theta = (\theta^1, \theta^2, \dots, \theta^n)$ is an n -dimensional parameter. The set S usually forms an n -dimensional differentiable manifold. For instance, a normal model $N(\mu, \sigma^2)$ forms a two-dimensional manifold with coordinates μ and σ . Such statistical manifolds usually have a metric-affine structure as well as a differentiable structure [1, 2]. The method of statistical manifolds is beginning to have fruitful developments in applications to nonlinear multivariable analysis, linear systems, time sequences, information theory, neural networks, and so on [3, 4]. Applications to physical systems are also beginning. In particular, parameter spaces of equilibrium systems such as the $T - \mu$ space of grand-canonical distributions have been investigated in detail. The investigations [5–10] showed that the Riemann curvature for various classical and quantum equilibrium systems diverges to infinity at phase transitions and also that stable systems, with no phase transitions, have small values of the curvature.

Recently we proposed two differential-geometrical approaches to the time evolution of non-equilibrium systems [11]. One approach depicts the evolution by the motion of a point in a statistical manifold, and the other one by the motion of a statistical manifold itself. We

showed that the Uhlenbeck–Ornstein process is a geodesic motion in the statistical manifold of negative constant curvature, and that a D -dimensional random walk (RW) is an expansion of a 2D sphere.

In the RW model, as a step time N increases, the sphere expands with the radius of $2\sqrt{N}$ from the singular state of zero radius to the flat sphere of infinite radius. In other words the curvature tensor fades away as $1/N$. We regarded this decrease behaviour of the curvature tensor as a geometrical representation of approach from an initial unstable state to a stable equilibrium state. This interpretation is consistent with the results of Ruppeiner [5], Janyszek *et al* [6–9] and Ginoza [10] for equilibrium systems: the curvature for stable equilibrium systems becomes small.

A walker of the RW model may move with step probabilities given at random, that is, with no correlation between steps. In reality we find correlated motion almost everywhere. Many correlated walk (CW) models appear in the literature. Their probability distribution functions are complicated, so it is very difficult to investigate corresponding statistical manifolds by analytical methods. In the present paper we develop a numerical method to calculate the curvature of a Riemann space associated with a CW model. The space is spanned by two parameters representing jump probabilities of the CW model.

A scenario of the scalar curvature R is as follows: the time development of the CW produces inhomogeneous expansion from a spherical surface of $R = \frac{1}{2}$ to a saddle surface of $R = -1$. The CW manifold starts at a point and changes to a one-dimensional manifold and then transforms to a two-dimensional spherical surface of $R = \frac{1}{2}$. The homogeneous space immediately deforms to an inhomogeneous space during the time development. A region of the space violently oscillates in time and the corresponding curvature is larger than that in other regions. Another region with no oscillations expands fast, that is, its curvature rapidly decreases. As a whole, the curvature of the space goes on decreasing, and soon becomes negative. Then the oscillations already start to fade away. The negative curvature goes on decreasing and finally the space converges to a homogeneous saddle surface of $R = -1$.

In what follows we first summarize a CW model and then calculate an associated statistical manifold, using a numerical method which is applicable to many other stochastic processes. Finally, we proceed to understand the scenario of the R above by physical terms. Key words are ‘stability’ and ‘order parameter’.

2. CW model

Our interest is not an application or generalization of CW models but a manifold associated with a CW model. According to a method in statistical geometry, a statistical model of a physical system produces a manifold with a metric-affine structure in general. To treat a correlated motion in a well defined manner, we follow a CW model [12–16]. The CW model is as follows.

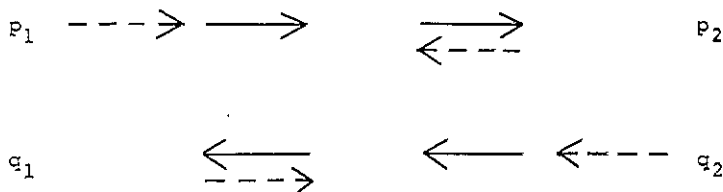


Figure 1. Step probabilities with correlations.

Suppose that a walker moves along a linear lattice of infinite extension right or left with given jump probabilities, which depend on the direction of the previous step. The right and left steps are called steps of type 1 and 2, respectively. If the last step is of type j , the probabilities of stepping right or left are denoted by p_j and q_j , with the normalization condition

$$p_j + q_j = 1 \quad j = 1, 2. \tag{1}$$

The definitions of the step probabilities are shown schematically in figure 1, where the steps in question are indicated by full arrows, and the last steps by broken arrows. The dynamics of the walker with correlated steps can also be represented in a square lattice. The walker's moves towards the left correspond to the upward moves of an object on the lattice. Let $P_j(X, Y)$ be the probabilities of the object arriving at the site (X, Y) with step-type j after N units of time. The probability of the object arriving at (X, Y) from any direction is $P(X, Y) = P_1(X, Y) + P_2(X, Y)$. Because of $X + Y = N$, we can regard P s as functions of X and N . The new function is denoted by $Q : Q_j(X, N) = P_j(X, Y)$, $Q(X, N) = P(X, Y)$. Consideration of two successive steps yields the following relations for P_j or Q_j :

$$\begin{aligned} Q_1(X, N) &= p_1 Q_1(X - 1, N - 1) + p_2 Q_2(X - 1, N - 1) & (X \geq 1, N \geq 1) \\ Q_2(X, N) &= q_1 Q_1(X, N - 1) + q_2 Q_2(X, N - 1) & (X \geq 0, N \geq 1). \end{aligned} \tag{2}$$

Let the walker be subject to the initial condition that it arrived at the origin with a right step:

$$Q_1(0, 0) = 1 \quad Q_2(0, 0) = 0 \tag{3}$$

The initial-value problem was exactly solved by Chen, Fujita, Okamura and others [12-16]. They used a generating function technique. The exact solution for $Q_j(X, N)$ is as follows:

$$\begin{aligned} Q_1(X, N) &= \begin{cases} \sum_{r=0}^X \binom{N-r-1}{X-1} \binom{X}{r} p_1^{X-r} q_2^{N-X-r} (p_2 - p_1)^r & (1 \leq X \leq N) \\ \delta_{0,N} & (X = 0) \end{cases} \\ Q_2(X, N) &= \sum_{r=0}^X \binom{N-r-1}{X} \binom{X}{r} p_1^{X-r} q_1 q_2^{N-X-r-1} (p_2 - p_1)^r \quad (0 \leq X \leq N). \end{aligned} \tag{4}$$

The combination number $\binom{M}{L}$ is defined as $M!/(M-L)!L!$ for $M \geq L \geq 0$, zero for the others.

Under the other initial conditions one can also solve the basic difference equation (2) through the same technique. Those exact solutions are unnecessary in the following. Note that the exact solution (4) is an alternating series in the parameter range $p_2 < p_1$. It is an easy exercise to ascertain that the exact solutions under the other initial conditions also are such alternating series in the same range. This characteristic will play a role in the dynamical behaviour of a statistical manifold associated with the correlated walk model.

The CW model and its generalized models were applied to the conformation of a polymer [17-19], the atomic diffusion in crystals with defects [19,20], and the non-equilibrium properties of a Lorentz gas [19,21], and so on (see references cited in [12-21]). Such applications or generalizations of the CW model are not our concern. Let us proceed to investigate a set of correlated walkers, that is, a statistical model.

3. Associated statistical manifold

3.1. Basic equations and numerical solutions

Now we investigate a geometrical structure of a statistical manifold associated with the CW model. Let S be a set of the probability functions $Q(X, N)$ parametrized by the jump probabilities p_j and q_j . Because of the normalization condition, each function $Q(X, N)$ in S is specified by a two-dimensional parameter $\theta = (\theta^1, \theta^2)$ such as $\theta = (p_1, q_2)$. Since $Q(X, N)$ is sufficiently smooth in θ , the set S has the structure of a two-dimensional manifold, where θ plays the role of a coordinate system.

A Riemann metric tensor can be naturally introduced in the manifold S :

$$g_{ij} = E(l(X, N)_{,i} l(X, N)_{,j}) = \sum_{X=0}^N \frac{1}{Q(X, N)} Q(X, N)_{,i} Q(X, N)_{,j} \quad (5)$$

where $l(X, N) = \ln Q(X, N)$ and $E(\cdot)$ stands for the expectation with respect to $Q(X, N)$ (see [2] or [11]). The subscripts following a comma are coordinate derivatives such as $\partial/\partial\theta^i$. The infinitesimal square distance $g_{ij} d\theta^i d\theta^j$ does not depend on the manner of parametrization θ of S . It is also invariant under a one-to-one transformation of the random variable X to another random variable, for instance the upward steps $Y = N - X$ on the square lattice or the displacement along the linear lattice $x = X - Y = 2X - N$.

The metric tensor produces a connection structure, which is prescribed by the Riemann-Christoffel connection coefficients:

$$\Gamma_{mkl} = \frac{1}{2}(g_{mk,l} + g_{ml,k} - g_{kl,m})$$

or

$$\Gamma_{ijk} = -\frac{1}{2} \sum_{X=0}^N \frac{1}{Q(X, N)^2} Q_{,i} Q_{,j} Q_{,k} + \sum_{X=0}^N \frac{1}{Q(X, N)} Q_{,i} Q_{,jk} \quad (6)$$

The connection structure gives the Riemann curvature tensor. Its covariant expression is given by

$$\begin{aligned} R_{ijkl} &= g_{im} R_{jkl}^m \\ &= g_{im} (\Gamma_{jl,k}^m - \Gamma_{jk,l}^m + \Gamma_{nk}^m \Gamma_{jl}^n - \Gamma_{nl}^m \Gamma_{jk}^n) \\ &= \Gamma_{ijl,k} - \Gamma_{ijk,l} + g^{mn} (\Gamma_{mil} \Gamma_{njk} - \Gamma_{mik} \Gamma_{njl}). \end{aligned} \quad (7)$$

Note that the third derivatives of $Q(X, N)$ in the $\Gamma_{ijl,k}$ and the ones in the $\Gamma_{ijk,l}$ cancel each other. Namely

$$\begin{aligned} \Gamma_{ijl,k} - \Gamma_{ijk,l} &= \sum_{X=0}^N \frac{1}{Q(X, N)} (Q_{,ik} Q_{,jl} - Q_{,il} Q_{,jk}) + \frac{1}{2} \sum_{X=0}^N \frac{1}{Q(X, N)^2} \\ &\quad \times (Q_{,i} Q_{,l} Q_{,jk} + Q_{,j} Q_{,k} Q_{,il} - Q_{,i} Q_{,k} Q_{,jl} - Q_{,j} Q_{,l} Q_{,ik}). \end{aligned} \quad (8)$$

The two-dimensional curvature tensor has only one independent component R_{1212} . The component is equivalent to the scalar curvature R , apart from a factor:

$$R = g^{ij} g^{kl} R_{ikjl} = 2(g^{11} g^{22} - g^{12} g^{21}) R_{1212} = 2 \det[g^{ij}] R_{1212}. \quad (9)$$

These geometrical quantities depend on the discrete time N as well as the coordinate θ , so the manifold S itself develops in time. We now have interest in the time development of local curvedness. Let us numerically evaluate the time evolution of the R at various coordinate values. First, by using the exact solution (4) and its first derivatives and second derivatives, we performed the numerical calculation in the quadruple precision of 16 bytes. But as the calculation for $p_1 > p_2$ and large N involves alternating series of extremely large terms, we could not obtain reliable results in such cases. So some calculations terminated before $N = 100$. To evade the problem, we successively solved the basic difference relations (2) and their derivatives step by step. We use the coordinate system (p_1, q_2) for a while. The coordinate system leads to the following derivatives with simple coefficients:

$$Q_1(X, N)_{,1} = Q_1(X - 1, N - 1) + p_1 Q_1(X - 1, N - 1)_{,1} + p_2 Q_2(X - 1, N - 1)_{,1}$$

$$Q_2(X, N)_{,1} = -Q_1(X, N - 1) + q_1 Q_1(X, N - 1)_{,1} + q_2 Q_2(X, N - 1)_{,1}$$

$$Q_1(X, N)_{,2} = -Q_2(X - 1, N - 1) + p_1 Q_1(X - 1, N - 1)_{,2} + p_2 Q_2(X - 1, N - 1)_{,2}$$

$$Q_2(X, N)_{,2} = Q_2(X, N - 1) + q_1 Q_1(X, N - 1)_{,2} + q_2 Q_2(X, N - 1)_{,2}$$

$$Q_1(X, N)_{,11} = 2Q_1(X - 1, N - 1)_{,1} + p_1 Q_1(X - 1, N - 1)_{,11} + p_2 Q_2(X - 1, N - 1)_{,11}$$

$$Q_2(X, N)_{,11} = -2Q_1(X, N - 1)_{,1} + q_1 Q_1(X, N - 1)_{,11} + q_2 Q_2(X, N - 1)_{,11} \quad (10)$$

$$Q_1(X, N)_{,12} = Q_1(X - 1, N - 1)_{,2} - Q_2(X - 1, N - 1)_{,1} + p_1 Q_1(X - 1, N - 1)_{,12} + p_2 Q_2(X - 1, N - 1)_{,12}$$

$$Q_2(X, N)_{,12} = -Q_1(X, N - 1)_{,2} + Q_2(X, N - 1)_{,1} + q_1 Q_1(X, N - 1)_{,12} + q_2 Q_2(X, N - 1)_{,12}$$

$$Q_1(X, N)_{,22} = -2Q_2(X - 1, N - 1)_{,2} + p_1 Q_1(X - 1, N - 1)_{,22} + p_2 Q_2(X - 1, N - 1)_{,22}$$

$$Q_2(X, N)_{,22} = 2Q_2(X, N - 1)_{,2} + q_1 Q_1(X, N - 1)_{,22} + q_2 Q_2(X, N - 1)_{,22}$$

Iterative calculation of the basic difference equations (2) and their derivatives (10) gives the R at each step N through equations (5)–(9). Of course, any other coordinate system should produce the same value of the scalar R .

We must exclude the values of the coordinates such that $Q(X, N)$ s become zero. The coordinate system (p_1, q_2) is defined in the range $0 < p_1 < 1$ and $0 < q_2 < 1$, in general. For instance, $Q(0, 2)$ and $Q(2, 2)$ are zero at $q_2 = 0$ and $p_1 = 0$, respectively (see equation (4), or equation (12) below). The $Q(0, 2)$ is zero also at $p_1 = 1$ under an initial

condition, $Q_2(0, 0) = 0$, and the $Q(2, 2)$ is zero also at $q_2 = 1$ under an initial condition, $Q_1(0, 0) = 0$.

We evaluated the R for many values of the coordinates under seven initial conditions: five initial conditions were independent of the coordinates and two conditions were dependent. Figure 2 displays the time development of the R at some typical coordinate values under three initial conditions:

- (i) $Q_1(0, 0) = 1$ $Q_2(0, 0) = 0$
 - (ii) $Q_1(0, 0) = 0.5$ $Q_2(0, 0) = 0.5$
 - (iii) $Q_1(0, 0) = p_2/(q_1 + p_2)$, $Q_2(0, 0) = q_1/(q_1 + p_2)$.
- (11)

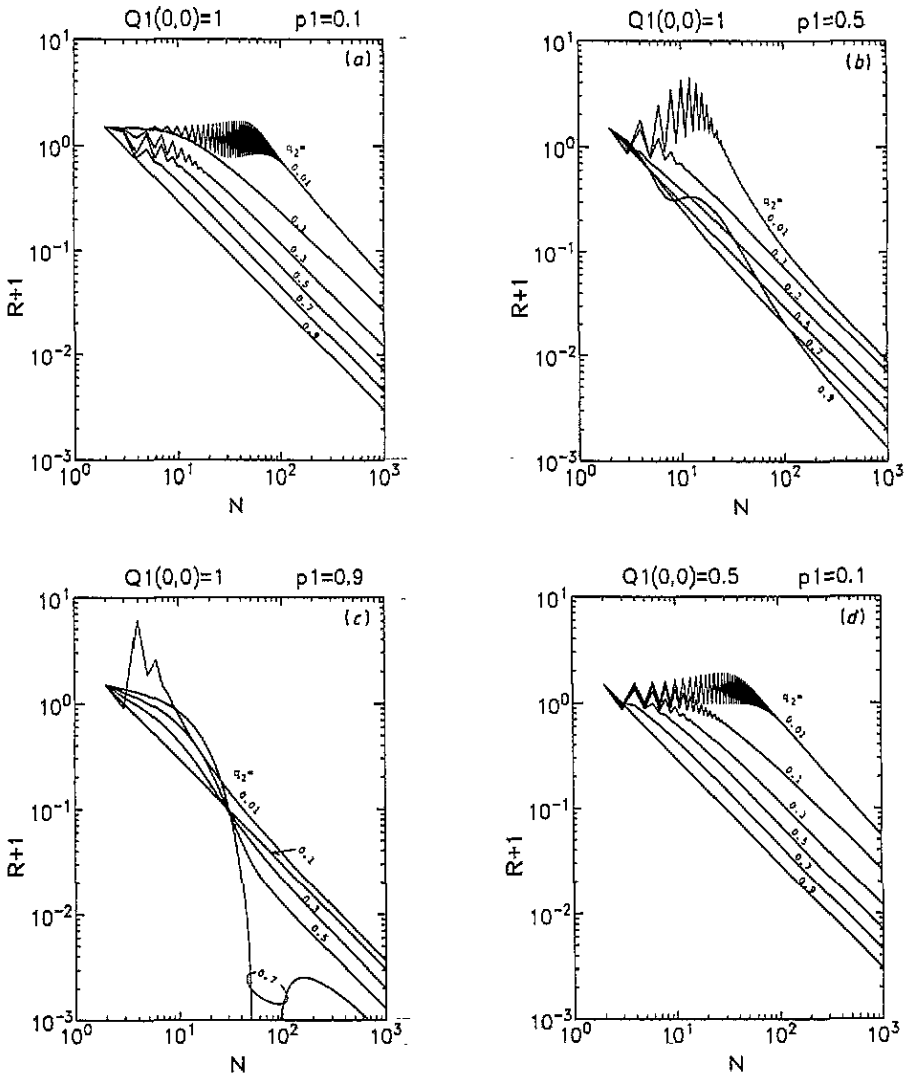


Figure 2. Step-time development of the scalar curvature R plus 1 at 1 at some typical coordinate values under initial conditions $Q_1(0, 0) = 1, 0.5, q_2/(p_1 + q_2)$. The coordinate p_1 and the initial condition are indicated at the top of each figure. The coordinate q_2 is shown for each curve.

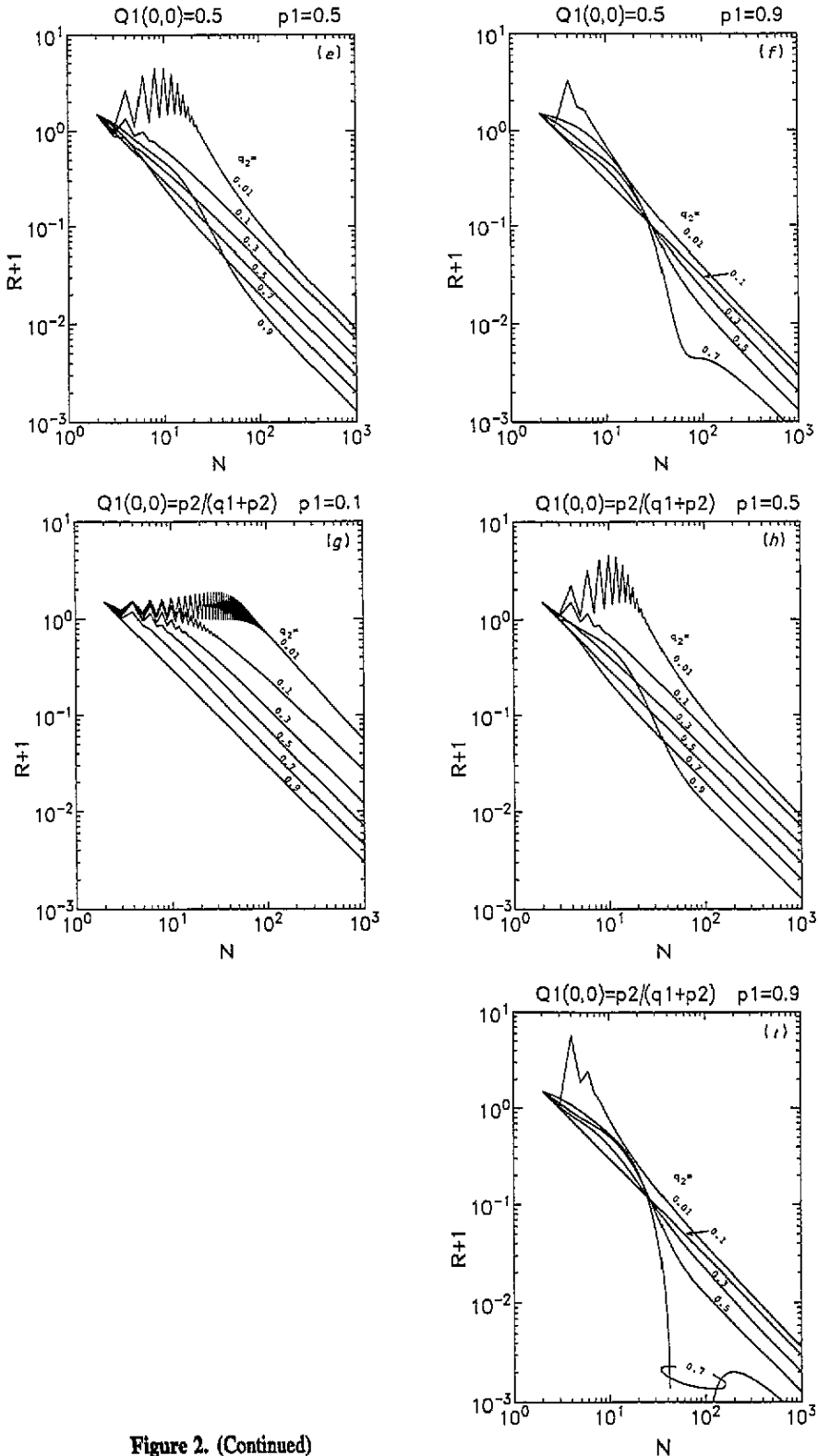


Figure 2. (Continued)

Here we omitted curves of $(p_1, q_2) \sim (1, 1)$, because most of the curves are out of the scale in figure 2. For instance, $R + 1$ at $(p_1, q_2) = (0.9, 0.9)$ under $Q_1(0, 0) = 1$ rapidly decreases and becomes zero at $N = 50$. The $R + 1$ is negative in $51 < N < 130$ and is of the order of 10^{-2} . After that it becomes positive and arrives at an extremum 1.0389×10^{-3} at $N = 120$. Later it monotonically decreases and finally approaches a straight line of gradient -1 .

3.2. Early behaviour

At $N = 0$ and 1, the two-dimensional scalar curvature R diverges to infinity by reason of degeneration to lower-dimensional manifolds. The probability function at $N = 0$, $Q(0, 0) = 1$, leads to $g_{11} = g_{22} = g_{12} = 0$. Hence the $N = 0$ manifold does not extend to any direction or it degenerates to a point.

At $N = 1$ the probability functions are given by

$$Q(0, 1) = q_1 Q_1(0, 0) + q_2 Q_2(0, 0) \quad Q(1, 1) = p_1 Q_1(0, 0) + p_2 Q_2(0, 0). \quad (12)$$

The two functions, of course, satisfy the normalization condition $Q(0, 1) + Q(1, 1) = 1$. It is possible to regard one of the two functions as a coordinate transformation, for instance, $\theta^1 = Q(0, 1)$. We then adopt a function independent of $Q(0, 1)$ as θ^2 . The new coordinate system results in $g_{11} = 1/[\theta^1(1 - \theta^1)]$, $g_{22} = g_{12} = 0$. Thus the $N = 1$ manifold has no extension to the θ^2 direction or it degenerates to a line.

At the first non-degenerate time $N = 2$, the manifold S has the constant positive curvature $R = \frac{1}{2}$. It is very cumbersome and troublesome to explicitly calculate geometrical quantities by using the coordinate system (p_1, q_2) or its linear transformation. It is convenient to choose as a coordinate system any two of the probability functions

$$\begin{aligned} Q(0, 2) &= q_1 q_2 Q_1(0, 0) + q_2^2 Q_2(0, 0) \\ Q(1, 2) &= (q_1 p_2 + p_1 q_1) Q_1(0, 0) + (p_2 q_1 + q_2 p_2) Q_2(0, 0) \\ Q(2, 2) &= p_1^2 Q_1(0, 0) + p_1 p_2 Q_2(0, 0). \end{aligned} \quad (13)$$

For instance, choice of $\theta^1 = Q(1, 2)$ and $\theta^2 = Q(2, 2)$ makes the probabilities reduce to simple expressions:

$$Q(0, 2) = 1 - \theta^1 - \theta^2 \quad Q(1, 2) = \theta^1 \quad Q(2, 2) = \theta^2. \quad (14)$$

These expressions produce the metric components as follows:

$$g_{11} = \frac{1}{1 - \theta^1 - \theta^2} + \frac{1}{\theta^1} \quad g_{22} = \frac{1}{1 - \theta^1 - \theta^2} + \frac{1}{\theta^1} \quad g_{12} = \frac{1}{1 - \theta^1 - \theta^2}. \quad (15)$$

It is a simple exercise to ascertain that the metric leads to $R = \frac{1}{2}$.

After $N = 2$, the time development of the R depends on the initial conditions. In an early period, $N \lesssim 100$, the behaviour is complicated. Nevertheless we can find a common feature independent of the initial conditions. The curvature oscillates in each region of $(p_1 = 0.1, q_2 < 0.9)$, $(p_1 = 0.5, q_2 < 0.5)$ and $(p_1 = 0.9, q_2 < 0.1)$. This suggests that the curvature oscillates in the region $p_1 + q_2 < 1$. We have ascertained that numerical data omitted here for many coordinate values and initial conditions also show the oscillation of the R in the region $p_1 + q_2 < 1$. We now note that the R in $p_1 + q_2 \ll 1$ violently

oscillates and also that its value is large as compared with that in other coordinate values. This oscillation corresponds to the fact that the exact solution (4) is an alternating series in the range $p_1 + q_2 < 1$, that is, $p_1 < p_2$. In a physical viewpoint the oscillation is thought to reflect the frequent flip-flop motions of such walkers, because $p_1 + q_2 \rightarrow 0$ is equivalent to $q_1 \rightarrow 1$ and $p_2 \rightarrow 1$; this means that the smaller the value of $p_1 + q_2$ is made, the more frequently the flip-flop steps occur. The larger curvature in $p_1 + q_2 \rightarrow 0$ is due to the fact that the localization of the probability function $Q(X, N)$ around the start site $x = X - Y = 0$ is unstable: in the limit state $(p_1, q_2) \rightarrow (0, 0)$, the walker stays forever at $x = 0$ or $x = \pm 1$, while in the other states the walker can diffuse to distant sites. Thus, a slight variation around the origin $(p_1, q_2) = (0, 0)$ produces a large change of the probability function. In other words the limit state $(p_1, q_2) \rightarrow (0, 0)$ is unstable. Thus the unstableness of the limit state is distinctly reflected by two properties of the statistical manifold: the curvature near the unstable state is larger than that of the other states and it also oscillates violently.

In an early period, $N \lesssim 50$, the curvature of a state around $(p_1, q_2) \sim (1, 1)$ rapidly decreases. The details depend on initial conditions, but the behaviour of rapid decreasing is an universal property. (Refer to the curves of $(p_1, q_2) = (0.9, 0.7)$ in figure 2. We also ascertained such behaviour at other states such as $(p_1, q_2) = (0.9, 0.9)$, which are omitted here.) This property can also be understood by interpreting the curvature as a measure of unstableness. At the start time a walker is localized at a point, $x = 0$. If the walker is specified by $(p_1, q_2) \sim (1, 1)$, it moves quickly out of the origin, as compared with other walkers. Hence its unstable motion near the start time produces a rapid change in the probability function $Q(X, N)$, and consequently the curvature is expected to vary by a large amount in time.

Thus, in early periods the walkers of $(p_1, q_2) \sim (1, 1)$ as well as $(p_1, q_2) \sim (0, 0)$ are unstable and the unstableness appears as the noticeable behaviour of the curvature.

3.3. Asymptotic behaviour

In $N \rightarrow \infty$, figure 2 suggests that the dependence of the R on the initial conditions disappears and that the R finally approaches a negative constant value -1 . In other words the R has the asymptotic form of

$$R \rightarrow -1 + \frac{h(p_1, q_2)}{N}. \tag{16}$$

The inhomogeneity $h(p_1, q_2)$ is almost independent of initial conditions. Around $N = 1000$ the deviation from $R = -1$ is less than 6×10^{-2} in the range $0.1 < p_1 < 0.9$ and $q_2 > 0.01$.

To examine characteristics of the small inhomogeneity $h(p_1, q_2)$ in the order of N^{-1} , we show details of the R at $N = 1000$ in figure 3, using the linear transformation

$$u = (p_1 + q_2)/2 \quad v = (p_1 - q_2)/2. \tag{17}$$

Note that for a fixed u the v varies in the range $-0.5 + |u - 0.5| < v < 0.5 - |u - 0.5|$. The full lines correspond to an initial condition, $Q_1(0, 0) = 1$, as is described in the caption, and the broken lines to another initial condition, $Q_1(0, 0) = 0.5$. Any broken line of $u < 0.8$ is omitted, because such a line coincides with the full line of the same coordinate value. The other initial conditions also produced similar behaviour, so we do not show their curves.

Does the independence on the initial conditions around $u = 0.9$ at $N = 1000$ mean that the N^{-1} term depends on initial conditions? To answer this question, we calculated the

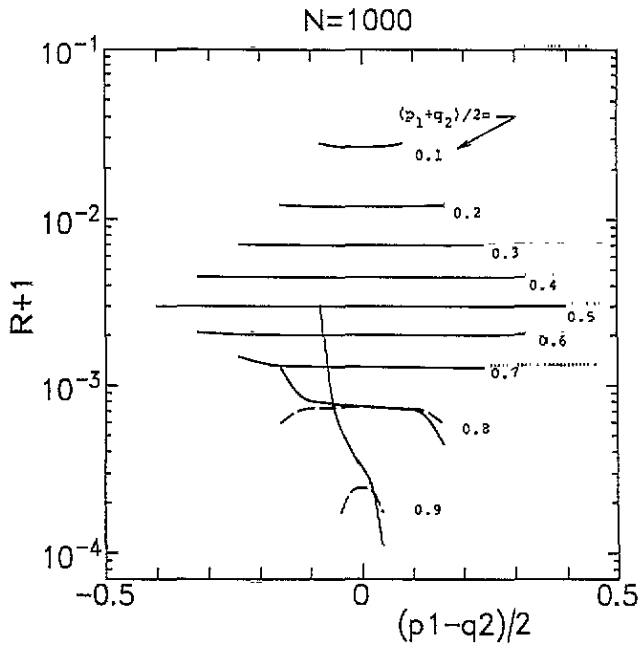


Figure 3. The right-left asymmetry $(p_1 - q_2)/2$ versus the scalar curvature R plus 1 at $N = 1000$ for various values of $(p_1 + q_2)/2$. The full lines correspond to $Q_1(0, 0) = 1$, and the broken lines to $Q_1(0, 0) = 0.5$.

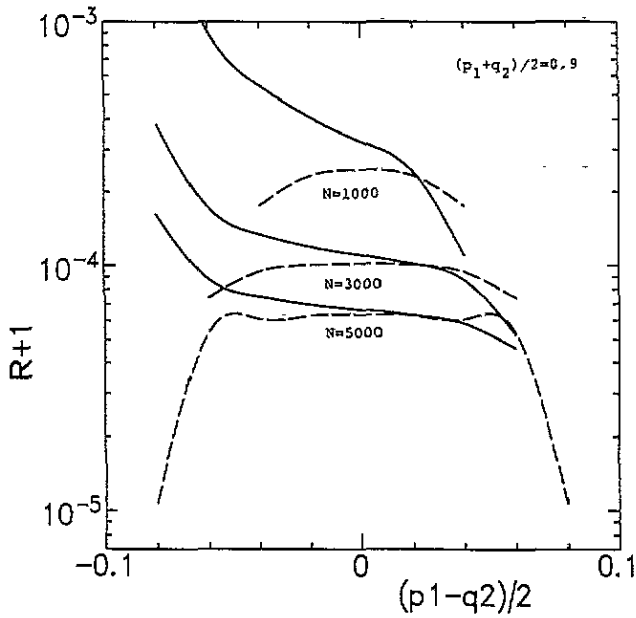


Figure 4. The right-left asymmetry $(p_1 - q_2)/2$ versus the scalar curvature R plus 1 at $N = 1000$, 3000 and 5000 for $(p_1 + q_2)/2 = 0.9$. The full lines correspond to $Q_1(0, 0) = 1$, and the broken lines to $Q_1(0, 0) = 0.5$.

curvature at later times. Figure 4 shows the curvature in the region $u = 0.9$ at three times, $N = 1000, 3000$ and 5000 , under two typical initial conditions $Q_1(0, 0) = 1, 0.5$. The full lines, $Q_1(0, 0) = 1$, gradually approach the broken lines, $Q_1(0, 0) = 0.5$. Hence we think that the initial condition dependence appearing in figures 3 and 4 is due to higher-order terms. Figure 4 also suggests that the two lines coincide with an almost horizontal line in $N \rightarrow \infty$. Accordingly we conclude that the inhomogeneity $h(u, v)$ in the N^{-1} term is:

- (i) independent of initial conditions;
- (ii) almost independent of the difference coordinate $v = (p_1 - q_2)/2$, representing the asymmetry between rightward steps and leftward steps;
- (iii) monotonically decreasing with respect to another coordinate $u = (p_1 + q_2)/2$, the mean of the diagonal components of the transition probabilities.

Note that the coordinate u represents the orderliness of walks. In fact, $u \rightarrow 1$ is equivalent to $p_2 \rightarrow 0$ and $q_1 \rightarrow 0$, so a walker of $u \sim 1$ tends to move almost without flip-flops. Namely it tends to walk smoothly and regularly. We may then regard the coordinate u as a 'regularity parameter' or an 'order parameter'. Hence the third property of the inhomogeneity function represents that the scalar curvature R is small for ordered states in the asymptotic time region.

4. Conclusions

We have investigated the time evolution of a statistical manifold associated with a CW model. We have found that the CW manifold evolves through some characteristic eras: it starts at a point and changes to a line and then transforms to a two-dimensional homogeneous space of the positive scalar curvature $R = \frac{1}{2}$. The space goes on deforming its form, oscillates partly, expands, and finally converges to a homogeneous space of the negative scalar curvature $R = -1$. In brief, the CW manifold inhomogeneously evolves from a spherical surface to a saddle surface. The relative decrease rate $-(1/R)(dR/dN) \rightarrow 1/N^2$ in large N is independent of an initial condition, and this rate is the same as that of a RW model [11]. (The RW manifold is always homogeneous and its curvature shows a simple behaviour such as $1/N$.) As in the RW model, we interpret the asymptotic decreasing behaviour of the curvature as a geometrical representation of the fact that a non-equilibrium system eventually proceeds from an initial unstable state to a stable equilibrium state. We have also pointed out that the large curvature, the violently oscillating curvature and the rapidly decreasing curvature in an early period are related to the unstableness of a state localized around a start site. Further, we have found that the asymptotic small inhomogeneity in a later period is independent of initial conditions and that the small inhomogeneity reflects the degree of orderliness of a walker's motion. Thus, we conclude that the curvature is a useful measure of stability and orderliness in non-equilibrium systems as well as in equilibrium systems. This interpretation of the R for non-equilibrium systems is consistent with Ruppeiner [5] and Janyszek's result [6-9] for equilibrium systems.

Some homogeneous statistical manifolds are already known: the normal distributions $N(\mu, \sigma^2)$, $R = -\frac{1}{2}$ [2] and classical ideal gases, $R = 0$ [5]. (For ideal bosons R is positive and inhomogeneous, and for ideal fermions R is negative and inhomogeneous [7].) The CW manifold converges to a saddle surface of $R = -1$.

Acknowledgment

We would like to thank a referee for indicating the importance of an initial condition depending on transition probabilities.

References

- [1] Rao C R 1945 *Bull. Calcutta Math. Soc.* **37** 81
- [2] Amari S 1985 *Differential-Geometrical Methods in Statistics (Lecture Notes in Statistics 21)* (Berlin: Springer)
- [3] Amari S 1992 *Bull. Jap. Soc. Ind. Appl. Math.* **2** 3
- [4] Amari S, Kurata K and Nagaoka H 1992 *IEEE Trans. Neural Networks* **3** 260
- [5] Ruppeiner G 1979 *Phys. Rev. A* **20** 1608
- [6] Janyszek H 1986 *Rep. Math. Phys.* **24** 1
- [7] Janyszek H and Mrugala R 1990 *J. Phys. A: Math. Gen.* **23** 467
- [8] Janyszek H 1990 *J. Phys. A: Math. Gen.* **23** 477
- [9] Janyszek H and Mrugala R 1989 *Phys. Rev. A* **39** 6515
- [10] Ginoza M 1991 *Oral presentation at the 1991 Spring Conference of Japan Physical Society*
- [11] Obata T, Hara H and Endo K 1992 *Phys. Rev. A* **45** 6997
- [12] Fujita S, Chen J T 1979 *Kinam* **1** 177
- [13] Chen J T, Okamura Y, Jacoby M and Fujita S 1979 *Acta Phys. Austr.* **51** 225
- [14] Okamura Y, Torres M, Blaisten-Barojas E and Fujita S 1981 *Acta Phys. Austr.* **53** 203
- [15] Okamura Y, Blaisten-Barojas E, Godoy S V, Ulloa S E and Fujita S 1982 *J. Chem. Phys.* **76** 601
- [16] Fujita S 1986 *Statistical and thermal physics part I. Probabilities and Statistics, Thermodynamics and Classical Statistical Mechanics* (Malabar, FL: Krieger) pp 39–56, 467–71
- [17] Chen J T, Okamura Y and Fujita S 1980 *J. Polym. Sci.: Polym. Phys. Ed.* **18** 175
- [18] Fujita S, Okamura Y and Chen J T 1980 *J. Chem. Phys.* **72** 3993
- [19] Fujita S 1986 *Statistical and thermal physics part II. Quantum Statistical Mechanics and Simple Applications* (Malabar: Krieger)
- [20] Okamura Y, Blaisten-Barojas E, Fujita S and Godoy S V 1980 *Phys. Rev. B* **22** 1638
- [21] Fujita S, Okamura Y, Blaisten E and Godoy S V 1980 *J. Chem. Phys.* **73** 4569